applied sciences

MDPI

Article

Green Recovery of Phenolic-Rich Extracts from Pineapple Crowns Using Deep Eutectic Solvents: FTIR Characterization and Chemometric Optimization

Ayşe Nur Ertaş [1], Zeynep Azra Akkın [1], Rabia Nur Bozkurt [1,2], İrem Toprakçı [2], Oana Cadar [3,*] and Selin Şahin [2,*]

[1] Department of Chemical Engineering, Faculty of Engineering and Natural Sciences, Istanbul Health and Technology University, 34445 Istanbul, Türkiye; ayse.ertas@istun.edu.tr (A.N.E.); zeynep.akkin@istun.edu.tr (Z.A.A.); rabia.bozkurt@istun.edu.tr (R.N.B.)
[2] Department of Chemical Engineering, Faculty of Engineering, Istanbul University-Cerrahpaşa, 34320 Istanbul, Türkiye; irem.toprakciyuksel@iuc.edu.tr
[3] INCDO-INOE 2000, Research Institute for Analytical Instrumentation, 67 Donath Street, 400293 Cluj-Napoca, Romania
* Correspondence: oana.cadar@icia.ro (O.C.); selins@iuc.edu.tr (S.Ş.)

Abstract

This study presents an integrated green analytical strategy combining deep eutectic solvent (DES) screening, Fourier transform infrared spectroscopy (FTIR), principal component analysis (PCA), and Box–Behnken response surface optimization for the valorization of pineapple crowns, an underexplored agro-industrial by-product. An ultrasound-assisted extraction (UAE) method was developed using DESs to obtain phenolic-rich extracts from pineapple (*Ananas comosus*) crowns. Five DES formulations were characterized by FTIR to evaluate their characteristic vibrational features, while extraction performance was assessed using total phenolic content (TPC) and antioxidant activity determined by the DPPH assay. Among the tested solvents, glycerol/urea (1:1, molar ratio) exhibited the highest extraction performance based on TPC and antioxidant activity measurements. PCA was used as a complementary tool to visualize the relationships among the DES formulations. Following preliminary temperature screening, 50 °C was selected for the optimization experiments. The extraction conditions were optimized using a Box–Behnken design coupled with response surface methodology (BBD–RSM), while desirability function analysis was applied to identify the optimum extraction conditions. The predicted optimum conditions were a sample mass of 1.09 g, an extraction time of 24.75 min, and a water content of 38.21%, yielding predicted responses of 34.66 mg GAE/g air-dried sample (ADS) for TPC and 12.30 mg Trolox equivalent antioxidant capacity (TEAC)/g-ADS for antioxidant activity. Experimental confirmation at the optimum showed deviations below 2% between predicted and observed responses, supporting the adequacy of the models. The quadratic models showed high goodness of fit (R^2 = 0.9871 for TPC, and R^2 = 0.9906 for antioxidant activity). Overall, the integration of DES-based UAE, FTIR characterization, PCA, and chemometric optimization provides a sustainable analytical approach for producing phenolic-rich extracts from pineapple crown biomass.

Keywords: deep eutectic solvents; antioxidant activity; phenolic compounds; PCA; chemometrics; green analytical chemistry

Academic Editors: Antonios E. Koutelidakis and Andrea Bassani

Received: 29 July 2026
Revised: 3 September 2026
Accepted: 10 September 2026
Published: 12 September 2026

1. Introduction

The development of environmentally friendly analytical methods has stimulated interest in extraction strategies that reduce the use of hazardous organic solvents, lower energy demand, and minimize analytical waste [1,2]. At the same time, large quantities of agricultural residues are generated worldwide each year, and much of this biomass remains underutilized. Agri-food waste is a significant natural resource rich in biologically active substances such as phenolics, carotenoids, vitamins and tocopherols [3]. Their conversion into value-added extracts can therefore contribute to circular-economy strategies while reducing the environmental burden associated with biomass disposal [4].

Pineapple (*Ananas comosus*) is widely cultivated in tropical regions and generates considerable quantities of biomass (crowns, peels, leaves and cores) during harvesting and processing [5–8]. Although pineapple crowns have been identified as a promising source of phenolic compounds and other bioactive constituents, most published studies have focused on compositional characterization, nutritional evaluation, and potential food or material applications of this by-product [8]. In contrast, studies investigating the extraction of phenolic compounds from pineapple crowns remain relatively scarce compared with those conducted on pineapple peels [9–13], pomace [14] and core [15–18]. Among pineapple processing residues, the crown represents a distinct and comparatively underexplored biomass fraction relative to more extensively investigated residues such as peel and stem. Its selection in the present study was therefore motivated by its potential for valorization and the limited information available on DES-assisted recovery of phenolic compounds from this specific biomass fraction, rather than by an assumption of superior extraction behavior compared with other pineapple residues.

Deep eutectic solvents (DESs) have emerged as promising alternative extraction media because of their low volatility, relatively simple preparation, and tunable physicochemical properties. DESs are generally prepared by combining two or more components at appropriate molar ratios to form a eutectic mixture with a melting point significantly lower than those of the individual constituents. Their extraction behavior depends on several interrelated properties, including polarity, viscosity, hydrogen-bonding capacity, and water content. Consequently, the performance of a DES cannot be predicted from its composition alone and should be evaluated experimentally for each plant matrix and analytical response. In DES-based extraction systems, water content is considered a critical operational parameter because it strongly influences the physicochemical properties of the solvent. The addition of water can reduce DES viscosity, improve mass transfer and modify solvent polarity, which facilitate the extraction of target compounds. However, excessive water might disrupt the hydrogen-bond network responsible for the unique properties of DESs and consequently reduce extraction efficiency. Therefore, optimization of water content is necessary to achieve the best extraction performance [19–21].

When combined with UAE, which enhances mass transfer through acoustic cavitation and promotes plant cell disruption, DESs provide a synergistic extraction strategy that improves the recovery of phenolic compounds through enhanced mass transfer and cell disruption induced by acoustic cavitation, while reducing extraction time and the use of hazardous organic solvents [21,22]. Nevertheless, the efficiency of DES-based UAE depends on both solvent composition and operational parameters. Consequently, solvent screening and systematic process optimization are required to establish suitable extraction conditions.

The development of a robust green extraction method requires a comprehensive evaluation of both solvent performance and process variables [23]. In this context, Principal Component Analysis (PCA) allows for the multivariate evaluation of the performance of different solvent systems, while Response Surface Methodology (RSM) is a powerful chemometric tool that enables the reliable determination of optimum extraction conditions

by reducing the number of experiments [24,25]. Among the experimental designs employed in response surface methodology, the Box–Behnken design (BBD) is one of the most widely used approaches for process optimization. BBD enables the efficient evaluation of linear, quadratic and interaction effects of multiple variables while requiring a relatively small number of experimental runs compared to full-factorial designs [26]. In addition, the BBD avoids experimental combinations where all factors are simultaneously set at their extreme levels, making it particularly suitable for optimizing extraction processes and predicting optimum operating conditions [27]. Fourier Transform Infrared Spectroscopy (FTIR) can further support the assessment of changes in the hydrogen-bonding environment after component mixing through shifts, broadening, and intensity changes in characteristic vibrational bands [28].

Previous studies have investigated DES-assisted extraction from agri-food matrices; however, the systematic screening and chemometric optimization of DES-based extraction from pineapple crowns remain limited. The present study therefore combines DES screening, FTIR characterization, PCA, temperature evaluation, and Box–Behnken response surface optimization to obtain phenolic-rich extracts from pineapple crown biomass. Five DES formulations were compared to assess the effects of solvent composition and molar ratio on extraction performance. Accordingly, the study aimed to develop and optimize a DES-based UAE process for pineapple crowns. Extraction performance was evaluated using total phenolic content and DPPH radical-scavenging activity, while temperature effects were assessed by one-way ANOVA followed by Tukey's post hoc test. PCA was used as a complementary tool for solvent comparison, while sample loading, extraction time, and DES water content were optimized by BBD–RSM. These mechanistic considerations were evaluated indirectly through extraction responses and FTIR observations rather than through direct measurement of DES physicochemical properties. Overall, the proposed approach provides a systematic framework for the resource-efficient valorization of pineapple crown biomass.

2. Materials and Methods

2.1. Materials

Fresh pineapple fruits were purchased from a local market in Zeytinburnu, Istanbul, Türkiye, in March 2026. Crowns were manually separated immediately after purchase, rinsed with tap water to remove visible impurities, immersed in a 1% (w/w) saline solution for 3–5 min to remove surface contaminants and rinsed twice with deionized water. The crowns were air-dried at room temperature until no further noticeable change in mass was observed (approximately 24 h). Moisture content was not determined separately. Therefore, the analytical results are expressed per gram of air-dried sample (ADS) rather than on a dry-matter basis. After air-drying, the crown material was manually fragmented into small pieces to obtain a more homogeneous sample and stored in airtight containers at −25 °C until further extraction experiments. No grinding procedure or particle-size classification was applied prior to extraction, which is a methodological limitation. Future studies should evaluate particle size as an additional process variable.

For the preparation of DESs, urea (≥99.5%) and lactic acid (90%) were purchased from Merck (Darmstadt, Germany), whereas glycerol (≥99.5%), L-proline (≥98.5%), and ammonium acetate (≥97%) were obtained from Sigma-Aldrich (St. Louis, MO, USA). For total phenolic content (TPC) determination, Folin–Ciocalteu reagent was purchased from Merck (Darmstadt, Germany), while sodium carbonate (Na_2CO_3, ≥99.5%) and gallic acid (≥99%) were obtained from Sigma-Aldrich (St. Louis, MO, USA). For antioxidant activity analysis using the DPPH radical scavenging assay, methanol (≥99.9%) was purchased from Merck (Darmstadt, Germany), whereas 2,2-diphenyl-1-picrylhydrazyl (DPPH) and Trolox

(≥97%) were obtained from Sigma-Aldrich (St. Louis, MO, USA). Deionized water used throughout the study was produced using a Milli-Q water purification system (Millipore, Bedford, MA, USA).

2.2. Preparation of Deep Eutectic Solvents

DESs were prepared by mixing the selected components at the molar ratios listed in Table 1. Glycerol/urea (1:1, 2:1 and 3:1), ammonium acetate/lactic acid (1:1), and L-proline/lactic acid (1:2) mixtures were heated at 80 °C under continuous magnetic stirring at 500 rpm for 60 min, until clear and homogeneous liquids were obtained [29]. No water was added during the initial preparation of the DESs. The prepared DESs were allowed to cool to room temperature and were stored in sealed containers until further use. Prior to the extraction experiments, the required water content was adjusted by adding the calculated amount of deionized water to the prepared DESs. The resulting mixtures were thoroughly homogenized before use.

Table 1. Composition and molar ratios of the prepared DESs.

DES No	Components	Molar Ratio
1	Glycerol/urea	1/1
2	Glycerol/urea	2/1
3	Glycerol/urea	3/1
4	Ammonium acetate/lactic acid	1/1
5	L-Proline/lactic acid	1/2

2.3. FTIR Analysis

FTIR spectra were recorded using a Tensor 27 spectrometer (Bruker, Billerica, MA, USA) equipped with an attenuated total reflectance (ATR) accessory over the range of 4000–400 cm^{-1}. Spectra were collected at a spectral resolution of 2 cm^{-1} using 32 scans per sample. A background spectrum was recorded prior to each sample measurement under the same instrumental conditions. Liquid DES samples were analyzed directly by placing an aliquot onto the ATR crystal, and the crystal surface was thoroughly cleaned between measurements. The spectra were used to examine changes in characteristic vibrational bands and the intermolecular interaction environment after component mixing.

2.4. Ultrasound-Assisted Extraction (UAE)

Ultrasound-assisted extraction (UAE) was performed based on previously reported UAE procedures for the recovery of phenolic compounds from pineapple by-products, with modifications [30]. The extraction was carried out using an ultrasonic bath (DK-600D, Shenzhen Dekang Electronic Cleaning Appliances Co., Ltd., Shenzhen, China) operating at a frequency of 40 kHz and a nominal equipment power of 180 W. The extraction temperature was set and monitored using the integrated temperature control system of the ultrasonic bath throughout the sonication process. During the preliminary experiments, 1.0 g of pineapple crown sample was mixed with 40 mL of extraction solvent and subjected to ultrasonic treatment for 30 min. The comparison of different DES systems was performed at 25 °C, whereas the effect of extraction temperature was evaluated at 25, 50, and 75 °C under otherwise identical extraction conditions. After extraction, the mixtures were filtered through a 0.45 μm membrane, and the filtrates were stored at 4 °C until analysis. All experiments were performed in triplicate as independent extraction experiments, and each replicate included the complete extraction and analytical procedure.

2.5. Total Phenolic Content (TPC) Analysis

TPC was determined using the Folin–Ciocalteu colorimetric method. Briefly, 20 µL of the extract was mixed with 380 µL of deionized water, followed by the addition of 2000 µL of Folin–Ciocalteu reagent and 1600 µL of sodium carbonate solution. The reaction mixture was incubated in the dark for 30 min, after which the absorbance was measured at 765 nm using a UV–Vis spectrophotometer (T60, PG Instruments Ltd., Leicestershire, UK). Corresponding DES blanks without pineapple crown extract were analyzed under the same assay conditions to account for background absorbance arising from the DES matrix and reagents. Gallic acid was used as the calibration standard, and the results were expressed as milligrams of gallic acid equivalents per gram of dry matter (mg-GAE/g-ADS) [31].

2.6. Antioxidant Activity (DPPH Assay)

The antioxidant activity was evaluated using the DPPH radical scavenging assay. Briefly, 100 µL of the extract was mixed with 600 µL of 80% methanol, followed by the addition of 3000 µL of DPPH solution prepared in 80% methanol. The reaction mixture was incubated in the dark for 30 min, and the absorbance was measured at 517 nm using a UV–Vis spectrophotometer. Trolox was used for calibration, and the results were expressed as milligrams of Trolox equivalent antioxidant capacity per gram of dry matter (mg TEAC/g-ADS) [32]. The Trolox calibration curve was constructed over the concentration range of 6.25–50 mg/L and was described by the equation $y = -0.00244x + 0.7521$ ($R^2 = 0.9987$).

DPPH radical scavenging activity was calculated as percentage inhibition using Equation (1) [33].

$$\text{DPPH inhibition } (\%) = \frac{A_0 - A_s}{A_0} \times 100 \quad (1)$$

where A_0 is the absorbance of the control and A_s is the absorbance of the sample.

For the preliminary DES and temperature screening experiments, DPPH radical-scavenging activity was expressed as percentage inhibition to facilitate direct comparison among the tested conditions. For the BBD-RSM experiments, antioxidant activity was quantified using the Trolox calibration curve and expressed as mg-TEAC/g-ADS as the response variable for optimization.

2.7. Box–Behnken Design-Response Surface Methodology (BBD-RSM)

Optimization of the UAE conditions was performed using response surface methodology (RSM) based on a three-factor, three-level Box–Behnken design (BBD). Sample mass (A), extraction duration (B), and water content of the DES (C) were selected as the independent variables, whereas TPC and antioxidant activity determined by the DPPH assay were considered the response variables. The total extraction solvent volume was kept constant at 40 mL throughout all BBD experiments. Thus, varying the sample mass effectively altered the solid-to-liquid ratio, allowing its influence on extraction performance to be evaluated while maintaining a constant solvent volume. The experimental design, model development, and statistical analyses were performed using Design-Expert software (Version 23.1.7.0, Stat-Ease Inc., Minneapolis, MN, USA). The adequacy and statistical significance of the developed models were evaluated by analysis of variance (ANOVA), considering the F-value, *p*-value, lack-of-fit test, coefficient of determination (R^2), adjusted coefficient of determination (adjusted R^2), predicted coefficient of determination (predicted R^2), coefficient of variation (C.V.), and adequate precision. The independent variables and their corresponding levels are summarized in Table 2. The ranges of the independent variables were selected based on preliminary experiments and previous studies on DES-based ultrasound-assisted extraction [19,20]. The selected levels were considered sufficiently broad to evaluate their effects on extraction performance while maintaining

practical operating conditions. In particular, the water-content range (20–50%) was chosen because water addition is known to modify DES viscosity, polarity, and hydrogen-bonding interactions, thereby influencing mass transfer and extraction efficiency.

Table 2. Levels of operational parameters used in the BBD-RSM.

Code	Independent Parameter	Level		
		Low	Medium	High
A	Sample mass (g)	0.5	1	1.5
B	Duration (min)	15	30	45
C	Water content (%)	20	35	50

2.8. Principal Component Analysis

Principal component analysis (PCA) was performed using Minitab Statistical Software (Version 22.2.1, Minitab LLC, State College, PA, USA) to evaluate the multivariate relationships among the experimental data [34]. PCA has been widely employed in chemometric studies of green extraction processes, including DES-based systems and response surface-designed experiments, to visualize patterns in multivariate datasets and to support process optimization [35,36].

PCA was conducted in two stages. First, the five DES formulations (DES1–DES5) were treated as observations, while TPC and antioxidant activity (AA) were used as variables to compare solvent performance.

2.9. One-Way ANOVA and Tukey's HSD Analysis

Statistical analyses were performed using Minitab Statistical Software 22 (Minitab Inc., State College, PA, USA). One-way analysis of variance (ANOVA) followed by Tukey's honestly significant difference (HSD) post hoc test was applied to compare the extraction performances of different DES formulations, and to evaluate the effect of extraction temperature on TPC and AA. Differences were considered statistically significant at $p < 0.05$. Pearson correlation analysis was also performed to evaluate the strength and direction of the linear relationship between TPC and AA. This analysis was used as a complementary statistical tool to assess whether variations in antioxidant activity were associated with changes in phenolic content across the tested extraction conditions. Pearson correlation coefficients (r) and corresponding *p*-values were calculated using Minitab Statistical Software (Version 22.2.1, Minitab LLC, State College, PA, USA).

3. Results and Discussion

3.1. FTIR Analysis of DESs

The molecular organization of the prepared DESs was evaluated by FTIR spectroscopy through comparison of the spectra of the individual components with those of the corresponding eutectic mixtures (Figure 1). Figure 1a presents the FTIR spectra of pure glycerol, urea, and glycerol/urea-based DESs prepared at molar ratios of 1/1 (DES1), 2/1 (DES2), and 3/1 (DES3). Pure glycerol exhibited a broad O–H stretching band centered at approximately 3283 cm^{-1}, together with characteristic C–H stretching vibrations at 2932 and 2878 cm^{-1}, a CH_2 bending vibration at 1414 cm^{-1}, and an intense C–O stretching band at approximately 1030 cm^{-1} [37,38]. In contrast, pure urea displayed characteristic N–H stretching vibrations at approximately 3426 and 3330 cm^{-1}, a prominent C=O stretching (amide I) band at 1672 cm^{-1}, and an N–H bending (amide II) band at 1586 cm^{-1}. The absorption bands at 1455, 1147, and 1044 cm^{-1} were mainly associated with C–N stretching vibrations and N–H deformation modes [39,40]. Following DES formation, the characteristic absorption bands of both parent components were retained, indicating that the fundamental chemical

structures of the parent components were preserved. However, systematic variations in band position and relative intensity were observed. The broad absorption band in the 3200–3400 cm^{-1} region shifted from 3338 cm^{-1} in DES1 to approximately 3258–3262 cm^{-1} in DES2 and DES3, suggesting that increasing the glycerol content progressively modified the intermolecular interaction environment within the eutectic mixtures. Likewise, the characteristic urea band at 1672 cm^{-1} shifted to 1625–1631 cm^{-1} following DES formation. A slight shift in this band toward higher wavenumbers from DES1 to DES3 further indicates that the molecular organization of the eutectic system was influenced by the glycerol-to-urea molar ratio. Although the C–O stretching band remained centered at approximately 1038–1040 cm^{-1} in all DESs, its relative intensity gradually increased as the glycerol content increased from DES1 to DES3. In contrast, no additional absorption bands appeared after mixing, supporting the formation of the eutectic mixtures through intermolecular interactions without the formation of new chemical species. Overall, the progressive spectral evolution observed from DES1 to DES3 demonstrates that varying the glycerol-to-urea molar ratio modulates the molecular organization of the eutectic mixtures while preserving the characteristic structural features of the constituent components.

Figure 1b compares the FTIR spectra of ammonium acetate, lactic acid, and the ammonium acetate/lactic acid-based DESs (DES4, 1/1). Pure lactic acid exhibited a broad O–H stretching band centered at approximately 3385 cm^{-1}, together with characteristic C–H stretching at 2987 cm^{-1}, a prominent C=O stretching band at 1717 cm^{-1}, and characteristic C–O stretching vibrations at approximately 1217 and 1122 cm^{-1} [41,42]. In contrast, ammonium acetate displayed characteristic N–H stretching and COO^- vibrational bands at approximately 2815, 1541, 1397, and 1013 cm^{-1} [42,43]. Following DES formation, the characteristic absorption bands of both parent components remained identifiable, indicating that the fundamental structural features of the starting materials were preserved. However, systematic variations in band position and relative intensity were observed. The broad O–H stretching band shifted from 3385 cm^{-1} to approximately 3225 cm^{-1} and became noticeably broader, suggesting a modified intermolecular interaction environment within the eutectic mixture. Likewise, the characteristic carbonyl stretching band of lactic acid at 1717 cm^{-1} became less pronounced, while a dominant absorption band appeared at approximately 1641 cm^{-1}. The characteristic ammonium acetate bands at 1541 and 1397 cm^{-1} were retained with slight shifts to 1561 and 1411 cm^{-1}, respectively. The characteristic absorption bands at approximately 1268, 1124, and 1040 cm^{-1} also remained evident in the DES spectrum, indicating that the principal vibrational features of the constituent components were preserved despite changes in their local molecular environment. The absence of additional absorption bands indicates that DES formation did not involve the generation of new chemical species but rather resulted from intermolecular interactions between the constituent components. Overall, the observed FTIR spectral changes demonstrate that these interactions influence the molecular organization of the eutectic mixture while preserving the characteristic structural features of the parent compounds.

Figure 1c compares the FTIR spectra of pure L-proline, lactic acid, and the L-proline/lactic acid-based DESs (DES5, 1/2). The characteristic FTIR bands of pure lactic acid were consistent with those described above. Pure L-proline exhibited characteristic absorption bands at approximately 1551 cm^{-1}, predominantly attributed to the asymmetric stretching vibration of the carboxylate (COO^-) group, together with bands at 1401–1375 cm^{-1} corresponding to the symmetric stretching vibration of the carboxylate group. The absorption bands observed in the 1288–1034 cm^{-1} region were mainly associated with C–N and C–O stretching vibrations, whereas the band at approximately 640 cm^{-1} was assigned to the rocking vibration of the CH_2 group in the pyrrolidine ring [44,45]. Following DES formation, the characteristic absorption bands of both parent components

remained identifiable, indicating that the fundamental structural features of the starting materials were preserved. However, systematic variations in band position and relative intensity were observed. The broad O–H stretching band was retained at approximately 3369 cm^{-1}, while the intense carbonyl stretching band of lactic acid at 1717 cm^{-1} became substantially less pronounced and a dominant absorption band appeared at approximately 1625 cm^{-1}. In addition, the characteristic absorption bands at approximately 1407, 1233, 1128, and 1044 cm^{-1} remained evident in the DES spectrum, indicating that the principal vibrational features of the constituent components were preserved despite changes in their local molecular environment. Overall, the observed spectral variations are consistent with the formation of the eutectic system while preserving the characteristic vibrational features of the constituent components.

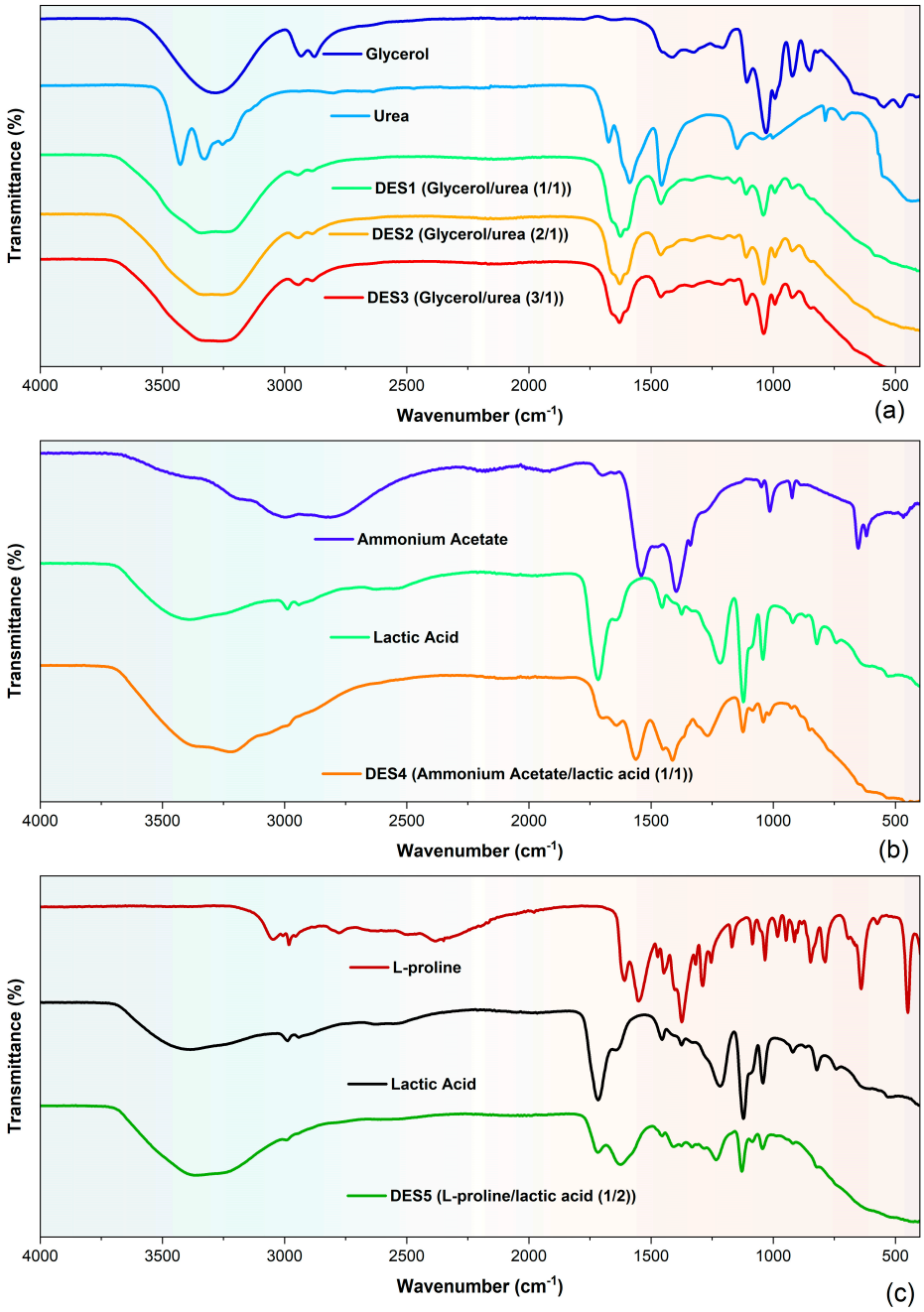

Figure 1. FTIR spectra of the *DESs* and their individual constituents: (**a**) glycerol/urea systems (DES1–DES3), (**b**) ammonium acetate/lactic acid (DES4), and (**c**) L-proline/lactic acid (DES5).

3.2. Preliminary Screening of DES Formulations

First, five DES formulations were evaluated to determine the most suitable extraction medium for pineapple crown phenolics. The extraction performances of the synthesized DESs were assessed based on TPC and DPPH radical scavenging activity. To determine whether the observed differences among the DES formulations were statistically significant, one-way ANOVA followed by Tukey's HSD post hoc test was performed.

One-way ANOVA revealed significant differences among the DES formulations in terms of total phenolic content ($p < 0.05$) (Table 3). Tukey's HSD multiple comparison test further demonstrated that the extraction efficiencies differed significantly between the solvents. DES1 (glycerol/urea, 1/1) exhibited the highest TPC (29.03 $\pm$ 0.002 mg GAE/g-ADS), whereas DES4 showed the lowest value (10.25 $\pm$ 0.001 mg GAE/g-ADS). The superior extraction performance of DES1 may be related to physicochemical characteristics previously reported for glycerol/urea-based DESs including favorable polarity, viscosity and hydrogen-bonding properties that may enhance the solubilization of phenolic compounds [46]. However, these properties were not experimentally determined in the present study, and therefore this explanation should be regarded as a literature-based interpretation rather than direct evidence. The fact that the glycerol/urea (1/1) system provides the highest total phenolic content indicates that the DES composition and the molar ratio of the components are decisive in the extraction efficiency. The superior performance of the glycerol/urea (1/1) system may be attributed to a favorable balance between polarity, viscosity, and hydrogen-bonding capacity. Phenolic compounds contain multiple hydroxyl groups that can interact with DES constituents through hydrogen-bonding interactions, enhancing their solubilization. Glycerol provides multiple hydroxyl functionalities and relatively low viscosity, while urea acts as an efficient hydrogen-bond acceptor that can promote interactions with phenolic compounds. At the 1/1 molar ratio, these properties appear to create a suitable extraction environment for the recovery of phenolic compounds from pineapple crowns. In contrast, increasing the glycerol proportion might alter solvent polarity and viscosity, thereby reducing mass transfer efficiency and extraction performance. However, since these properties were not directly measured in the present study, this interpretation remains tentative. Liu et al. also compared eight different DES formulations (choline chloride/lactic acid, choline chloride/ethylene glycol, choline chloride/glycerol, choline chloride/sucrose, choline chloride/citric acid, choline chloride/urea, glycerol/urea and L-proline/glycerol), where glycerol/urea exhibited the highest total phenolic content among all tested solvents [47]. The authors attributed this superiority to the polyol nature of glycerol, which reduces solvent viscosity and improves solvent extensibility. Furthermore, although both glycerol/urea and choline chloride/urea contained urea, replacing glycerol with choline chloride resulted in the lowest extraction efficiency. This shows the critical role of DES composition in phenolic extraction. Similarly, Vidić et al. reported that NADES components significantly affect the extraction efficiency of phenolic compounds by altering the polarity, viscosity and hydrogen bond interactions of the solvent [48]. On the other hand, the decrease in TPC with increasing glycerol content (DES2 and DES3) may be due to increased solvent viscosity and changes in polarity. The literature also reports that DES component ratios alter the physicochemical properties of the solvent, affecting the solubility and extraction efficiency of phenolic compounds [48]. Similarly, Nascimento et al. reported that the 2/1 and 1/2 molar ratios in the glycerol/urea system did not show sufficient physicochemical stability [49]. Therefore, the 1/1 ratio of glycerol/urea was preferred due to the fact that it formed a homogeneous and stable DES.

Table 3. Comparison of total phenolic content and antioxidant activity of pineapple crown extracts obtained using different DES formulations. Values are expressed as mean ± SD (n = 3). Different lowercase letters in each column indicate significant differences according to Tukey's HSD test ($p < 0.05$).

DES	TPC (mg-GAE/g-ADS)	AA (Inhibition %)
DES1	29.03 ± 0.002 [a]	88.97 ± 0.003 [a]
DES2	22.28 ± 0.002 [b]	86.24 ± 0.004 [b]
DES3	19.21 ± 0.001 [c]	88.22 ± 0.002 [a]
DES4	10.25 ± 0.001 [e]	58.46 ± 0.001 [d]
DES5	16.76 ± 0.000 [d]	72.14 ± 0.004 [c]

On the other hand, the comparatively lower TPC obtained with the lactic-acid-based DES formulations may also be related to their acidic chemical environment. The ionization state of phenolic acids and flavonoid hydroxyl groups can influence their solubility and interactions with the DES components, while the hydrogen-bonding environment of organic-acid-based DES may further affect solute-solvent affinity [50]. Nevertheless, this explanation should be regarded as a possible mechanistic interpretation rather than direct experimental evidence, since the pH and other physicochemical properties of the prepared DES formulations were not directly measured and individual phenolic compounds were not identified.

DES1 and DES3 belonged to the same Tukey group for antioxidant activity, indicating no significant difference between their mean inhibition values ($p > 0.05$). However, DES1 exhibited the highest TPC and showed the highest mean antioxidant activity among the tested DES formulations. Therefore, DES1 was selected for further study based on the combined consideration of both response variables rather than statistical superiority in antioxidant activity alone. A strong positive trend was remarked between TPC and antioxidant activity (r = 0.874), although the relationship did not reach statistical significance ($p = 0.053$), likely in part because only five DES formulations were evaluated. The similar antioxidant responses of DES1 and DES3 despite their different TPC values may reflect differences in extract composition [51]. However, this explanation remains tentative because the phenolic profile was not characterized.

DES1 was selected for further investigation based on the statistical evaluation. Subsequently, the influence of extraction temperature on its extraction performance was examined prior to chemometric optimization.

3.3. Effect of Extraction Temperature on DES1 Extraction Performance

To further improve the extraction efficiency, the influence of extraction temperature was investigated using the selected DES1 (glycerol/urea, 1/1). Temperature is one of the most influential parameters in UAE, as it directly affects solvent viscosity, diffusion rate and mass transfer between the plant matrix and the extraction medium. The extraction performance was evaluated in terms of TPC and AA (Table 4).

The extraction temperature significantly influenced both TPC and antioxidant activity ($p < 0.05$), as seen in Table 4. Increasing the temperature from 25 to 50 °C significantly enhanced the TPC from 29.03 to 33.05 mg GAE/g-DM, and increased the antioxidant activity from 88.97% to 91.71%. This improvement is consistent with lower solvent viscosity and enhanced mass transfer at moderate temperature. On this basis, 50 °C was selected for the subsequent optimization. The decrease in TPC and antioxidant activity observed at 75 °C may indicate that the beneficial effect of increased temperature on mass transfer was offset by temperature-dependent changes in some extractable antioxidant constituents.

Possible mechanisms include thermal degradation, oxidation or structural transformation of heat-sensitive phenolic compounds [52]. However, since individual phenolic compounds and their thermal stability were not directly investigated in the present study, a specific degradation mechanism cannot be established from the current data.

Table 4. Influence of extraction temperature on the extraction efficiency of DES1 evaluated by total phenolic content and antioxidant activity. Values are expressed as mean ± SD (n = 3). Different lowercase letters in each column indicate significant differences according to Tukey's HSD test ($p < 0.05$).

Temperature (°C)	TPC (mg-GAE/g-ADS)	AA (Inhibition %)
25	29.03 ± 0.002 ^{b}	88.97 ± 0.003 ^{b}
50	33.05 ± 0.003 ^{a}	91.71 ± 0.002 ^{a}
75	27.92 ± 0.002 ^{c}	80.09 ± 0.002 ^{c}

3.4. PCA Analysis of DES Formulations

PCA was applied to TPC and antioxidant activity data from the five DES formulations. The first two principal components explained 100% of the variance, with PC1 accounting for 96.8% and PC2 for 3.2%. Thus, differences among the DES formulations were represented predominantly along PC1.

Figure 2a shows a score plot where the DES formulations are clearly separated by their extraction characteristics. Meanwhile, DES1, DES2 and DES3 synthesized from glycerol and urea with varying molar ratios were found on the positive side of PC1, while DES4 and DES5, in which lactic acid acted as the hydrogen bond donor, were situated on the negative side. This distribution is in good agreement with the experimental results where the glycerol/urea-based DESs showed greater TPC and AA values than the lactic acid-based systems. As shown in Table 3, the highest TPC and AA values of the examined DES formulations were obtained for DES1, whilst the lowest responses were found for DES4. Among the solvents studied, DES1 was clearly separated from the other formulations, which indicates its higher extraction performance. The biplot (Figure 2b) gave further insight into the links between the response variables and the DES formulations. TPC and AA demonstrated the same positive loading on PC1 (0.707), suggesting that both responses contributed equally to the first main component and varied in the same direction. Thus, PC1 is considered as the total performance of the extraction of the DES systems. Conversely, the opposite loadings obtained for PC2 (TPC = −0.707 and AA = 0.707) suggest that this component is mainly related to the small variation between the two response variables. However, PC2 only contributed approximately 3.2% of the overall variation and hence contributed little in differentiating the DES formulations.

TPC and antioxidant activity loaded in the same direction on PC1, indicating that both responses followed a broadly similar pattern across the five DES formulations. This result is consistent with the positive Pearson correlation (r = 0.874), although the association was not statistically significant (p = 0.053). PCA should therefore be regarded as an exploratory visualization of solvent performance rather than independent confirmation of a significant relationship.

Overall, the PCA pattern was consistent with the experimental screening results: glycerol/urea-based DESs were located in the higher-response region, and DES1 provided the most favorable combination of TPC and antioxidant activity. DES1 was therefore selected primarily on the basis of the measured responses, with PCA used as complementary support. Temperature screening subsequently showed that 50 °C gave the highest TPC

and antioxidant activity among the conditions tested (Table 4); DES1 and 50 °C were consequently used in the Box–Behnken optimization.

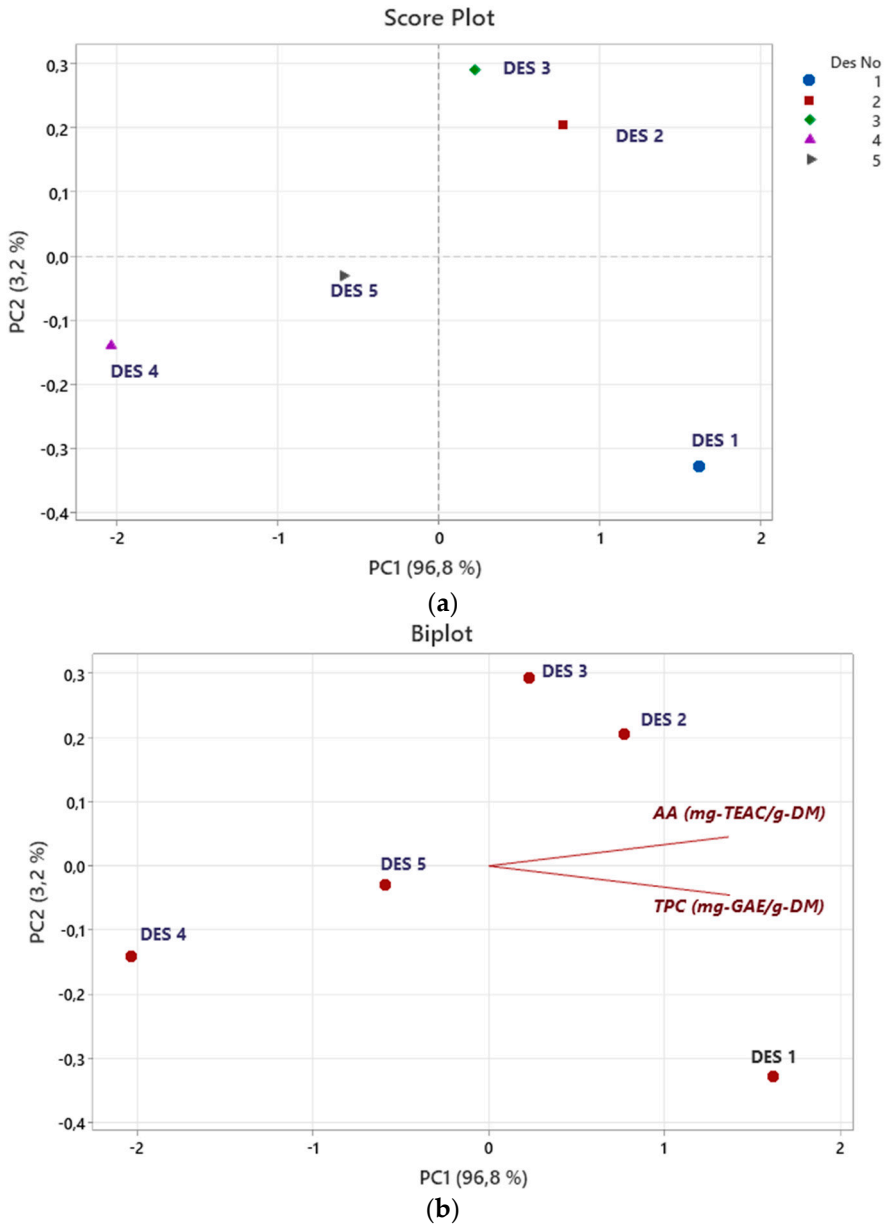

Figure 2. Principal component analysis (PCA) of the DES formulations: (**a**) score plot and (**b**) biplot showing the relationships between the DES formulations and the response variables (TPC and AA).

Given the limited number of DES formulations ($n = 5$) and response variables (TPC and antioxidant activity), the PCA should be interpreted strictly as an exploratory visualization rather than as an independent confirmatory statistical analysis. Accordingly, the selection of DES1 for subsequent optimization was based primarily on the experimentally measured extraction responses, while PCA was used only to provide a complementary visualization of the relationships among the tested solvent systems.

3.5. Box–Behnken Design and Response Surface Analysis

The BBD–RSM comprised 17 experimental runs (Table 5). TPC ranged from 24.24 to 35.18 mg GAE/g-DM, while antioxidant activity ranged from 6.07 to 12.40 mg TEAC/g-DM, providing sufficient response variation for quadratic modelling.

Table 5. Experimental data obtained through the Box–Behnken design–response surface methodology (BBD-RSM).

Run	Factor 1 A: Sample Mass (g)	Factor 2 B: Duration (min)	Factor 3 C: Water Content (%)	Response 1 TPC (mg-GAE/g-ADS)	Response 2 AA (mg-TEAC/g-ADS)
1	1	15	50	29.562	11.98
2	1	30	35	34.207	11.938
3	1	30	35	34.895	10.963
4	1.5	30	20	24.241	10.575
5	1	30	35	35.184	12.016
6	1.5	15	35	29.901	12.398
7	1	15	20	28.918	11.327
8	0.5	15	35	30.947	6.11
9	1	30	35	34.873	11.843
10	1	45	20	24.886	10.506
11	1.5	45	35	24.923	10.025
12	0.5	30	20	27.215	6.108
13	1	45	50	30.407	10.69
14	0.5	30	50	33.837	6.071
15	0.5	45	35	32.724	6.084
16	1.5	30	50	28.212	11.018
17	1	30	35	34.873	11.785

The fitted quadratic polynomial equations describing the effects of the independent variables on TPC and AA are presented in Equations (2) and (3), respectively:

$$TPC = +34.81 - 2.18A - 0.7985B + 2.09C - 1.69AB - 0.6628AC + 1.22BC - 2.62A^2 - 2.56B^2 - 3.81C^2 \quad (2)$$

$$AA = +11.71 + 2.46A - 0.5638B + 0.1554C - 0.5867AB + 0.1200AC - 0.1173BC - 2.87A^2 - 0.1860B^2 - 0.3972C^2 \quad (3)$$

The regression coefficients describe the direction and relative magnitude of each model term within the experimental domain. Positive coefficients indicate an increase in the response, whereas negative coefficients indicate a decrease. Both quadratic models were highly significant ($p < 0.0001$; Table 6). Although the lack of fit for the TPC model was not statistically significant ($p = 0.0535$), its proximity to the conventional significance threshold ($p = 0.05$) suggests that the model adequacy should be interpreted cautiously rather than solely on the basis of statistical non-significance. Nevertheless, the high R^2, low coefficient of variation, model significance and close agreement between the predicted and experimentally validated optimum response (<2% deviation) collectively support the practical adequacy of the quadratic model within the investigated experimental domain.

Regarding TPC, the linear effects of sample mass (A), extraction duration (B) and water content (C) were all significant ($p < 0.05$). Among the interaction terms, AB and BC significantly affected TPC, whereas AC was not significant ($p > 0.05$). In addition, all quadratic terms (A^2, B^2 and C^2) were significant at $p < 0.0001$. Equation (2) also supports this finding. The significant negative quadratic coefficients (A^2, B^2 and C^2) suggest that the responses exhibited pronounced curvature, indicating the existence of optimum extraction conditions rather than a simple linear relationship. This demonstrates that there is a pronounced curvature in the response surface. Therefore, the relationship between the variables is explained by quadratic models (Equation (2)) instead of linear models [53].

Table 6. Analysis of variance test for quadratic models.

	Source	Sum of Squares	df	Mean Square	F-Value	*p*-Value	Significance
TPC	Model	228.02	9	25.34	59.57	<0.0001	Significant
	A: Sample mass	38.05	1	38.05	89.45	<0.0001	
	B: Duration	5.10	1	5.10	11.99	0.0105	
	C: Water content	35.10	1	35.10	82.54	<0.0001	
	AB	11.41	1	11.41	26.82	0.0013	
	AC	1.76	1	1.76	4.13	0.0816	
	BC	5.95	1	5.95	13.98	0.0073	
	A^2	29.01	1	29.01	68.21	<0.0001	
	B^2	27.55	1	27.55	64.77	<0.0001	
	C^2	60.97	1	60.97	143.35	<0.0001	
	Residual	2.98	7	0.4253			
	Lack of fit	2.46	3	0.8195	6.32	0.0535	Not significant
	Pure error	0.5186	4	0.1296			
	Cor total	231.00	16				
AA	Model	88.95	9	9.88	82.01	<0.0001	Significant
	A: Sample mass	48.23	1	48.23	400.23	<0.0001	
	B: Duration	2.54	1	2.54	21.10	0.0025	
	C: Water content	0.1931	1	0.1931	1.60	0.2460	
	AB	1.38	1	1.38	11.43	0.0118	
	AC	0.0576	1	0.0576	0.4780	0.5116	
	BC	0.0550	1	0.0550	0.4563	0.5210	
	A^2	34.65	1	34.65	287.55	<0.0001	
	B^2	0.1457	1	0.1457	1.21	0.3079	
	C^2	0.6645	1	0.6645	5.51	0.0512	
	Residual	0.8436	7	0.1205			
	Lack of fit	0.1166	3	0.0389	0.2139	0.8822	Not significant
	Pure error	0.7269	4	0.1817			
	Cor total	89.79	16				

For antioxidant activity, the linear effects of sample mass (A) and extraction duration (B) were significant ($p < 0.05$), whereas water content (C) was not. Among the interaction terms, only AB was significant. Moreover, only the quadratic effect of sample mass (A^2) significantly contributed to the model, suggesting that antioxidant activity was primarily controlled by sample loading rather than by water content within the investigated experimental range. Likewise, the negative quadratic coefficient of A^2 indicates that excessive sample mass adversely affected antioxidant activity beyond the optimum level (Equation (3)). Although some individual model terms were not statistically significant ($p > 0.05$), they were retained to preserve the hierarchical structure of the quadratic response surface models.

The statistical parameters further confirmed the adequacy and predictive capability of the developed models (Table 7). The coefficients of determination (R^2) values were 0.9871 and 0.9906 for TPC and AA, respectively. This means that more than 98% of the experimental variability was explained by the fitted quadratic models. The adjusted R^2 and predicted R^2 values were also in reasonable agreement, suggesting satisfactory predictive performance without substantial overfitting. Furthermore, the low coefficients of variation (C.V.) of 2.13% for TPC and 3.44% for AA demonstrate good experimental precision and reproducibility. C.V. values below 10% are generally considered indicative of reliable models in response surface methodology studies [54,55].

Table 7. Statistical data for response variables.

Response	SD	R^2	R_A^2	R_P^2	C.V. (%)
TPC	0.6522	0.9871	0.9705	0.8262	2.13
AA	0.3471	0.9906	0.9785	0.9666	3.44

SD = standard deviation; R_A^2 = adjusted R^2; R_P^2 = predicted R^2, C.V.= coefficient of variation.

Furthermore, the interactions among the extraction variables were visualized using three-dimensional (3D) response surface plots (Figures 3 and 4). The curved response surfaces observed for both responses are consistent with the significant quadratic terms identified by ANOVA test (Table 6). Figure 3a illustrates the combined effects of sample mass and extraction duration on TPC, while water content was maintained at its center level. TPC increased as both variables approached intermediate levels and reached its maximum at approximately 1.0 g sample mass and 25–30 min extraction time. Further increases in either variable resulted in a decline in TPC, producing a dome-shaped response surface. This pattern agrees with the significant quadratic terms identified by ANOVA. The decline at higher solid loading or longer sonication may reflect reduced solvent availability per unit mass or changes in susceptible extract constituents during prolonged treatment [56–58]. The significant AB interaction indicates that the effect of extraction duration depended on the sample mass used during extraction. At lower sample masses, extending the extraction time facilitated solvent penetration and mass transfer, thereby enhancing phenolic recovery. In contrast, at higher sample masses, prolonged extraction did not result in proportional increases in TPC, likely because of reduced solvent availability per unit mass and limitations in mass-transfer efficiency. This interaction highlights the importance of balancing solid loading and extraction duration to maximize extraction performance.

Figure 3b demonstrates that both sample mass and water content markedly affected TPC. Increasing water content initially enhanced phenolic extraction, whereas excessive sample mass reduced the extraction efficiency as explained above [58,59]. The curved response surface suggests that an appropriate balance between solvent composition and solid loading is required to maximize phenolic recovery. As seen in Figure 3c, the interaction between extraction duration and water content also exhibited a curved response surface. Moderate extraction durations combined with intermediate water contents produced the highest TPC values, whereas prolonged extraction reduced phenolic recovery despite increasing water content. This reduction might be associated with oxidation or degradation of phenolic compounds during extended sonication [58]. The improvement at intermediate water contents may reflect reduced DES viscosity and changes in polarity and hydrogen-bonding interactions, which favor mass transfer and solubilization. Excess water, however, may weaken the DES network and lower extraction efficiency. Comparable behavior has been reported for ultrasound-assisted DES systems [56]. Hence, the optimum water content predicted by the model (38.21%) likely represents a balance between two competing effects. Moderate water addition decreases DES viscosity, thereby improving solvent penetration into the plant matrix and enhancing mass transfer during ultrasound-assisted extraction. However, excessive dilution can weaken the hydrogen-bonding network responsible for the unique solvation properties of the DES, leading to reduced solubilization of phenolic compounds. So, the optimum identified in this study appears to reflect a compromise between enhanced diffusivity and preservation of favorable solvent–analyte interactions.

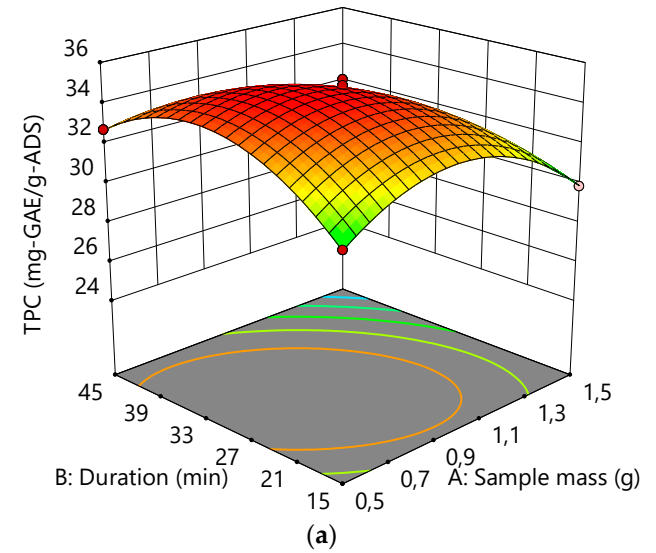

(**a**)

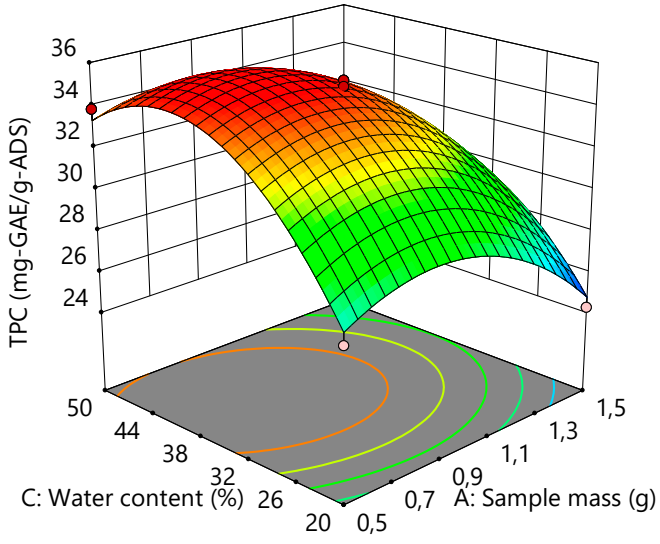

(**b**)

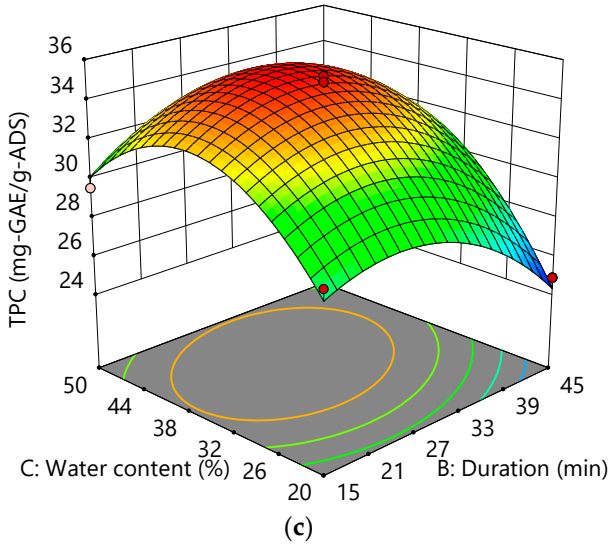

(**c**)

Figure 3. Three-dimensional response surface plots showing the interactive effects of (**a**) sample mass and extraction duration, (**b**) sample mass and water content, and (**c**) extraction duration and water content on TPC.

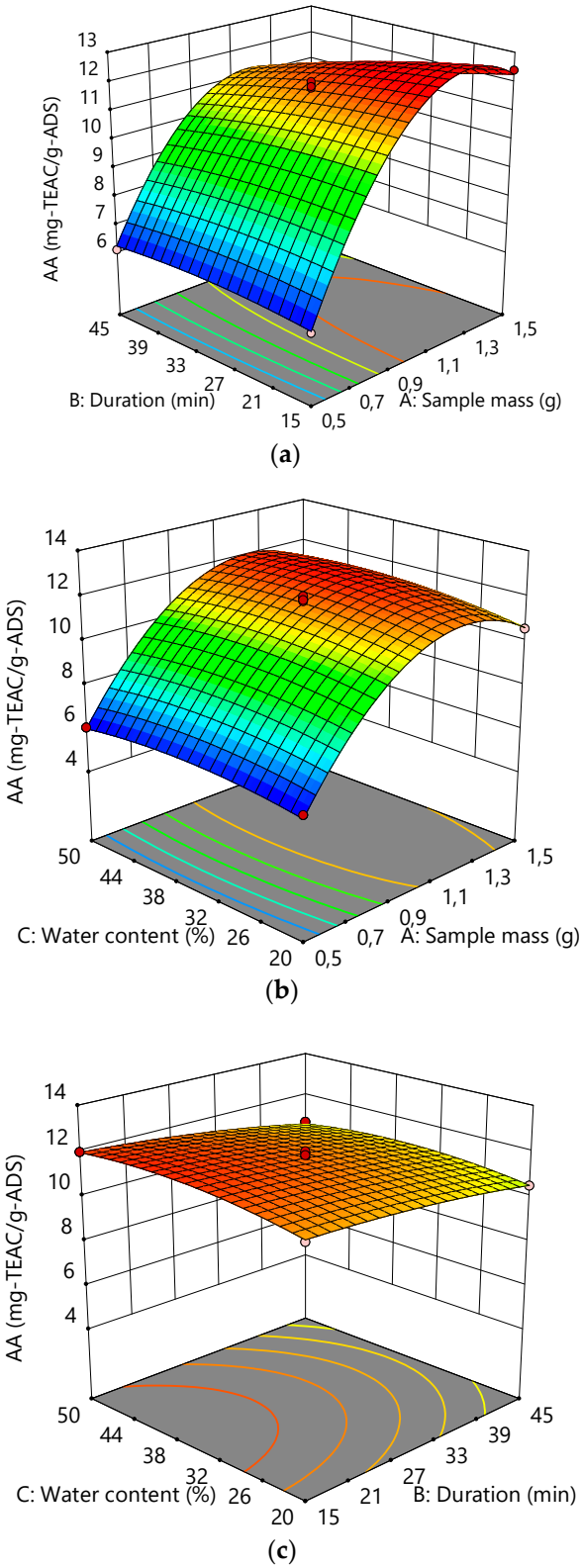

Figure 4. Three-dimensional response surface plots illustrating the interaction effects of (**a**) sample mass (A) and extraction duration (B), (**b**) sample mass (A) and water content (C), and (**c**) extraction duration (B) and water content (C) on the AA.

On the other hand, the significant BC interaction indicates that the influence of extraction time was dependent on the water content of the DES. Moderate water contents may reduce solvent viscosity and improve diffusivity, thereby enhancing extraction during

shorter and intermediate extraction times. However, under prolonged extraction conditions, excessive exposure to ultrasound together with changes in solvent structure may reduce phenolic recovery. This interaction highlights the importance of balancing extraction duration and DES composition to maximize extraction efficiency.

Figure 4a shows that antioxidant activity was primarily governed by sample mass. AA increased regularly with increasing sample mass until reaching an optimum region. Then, AA tended to slightly decrease. This observation is consistent with the highly significant linear and quadratic effects of sample mass identified by the ANOVA test (Table 6). The significant AB interaction observed for antioxidant activity suggests that the influence of extraction duration varied according to sample loading. Increasing extraction time was more beneficial at moderate sample masses, whereas at higher sample masses the improvement in antioxidant activity became less pronounced. This behavior may be associated with limitations in cavitation efficiency and solvent penetration at higher solid loadings, which can reduce the effectiveness of prolonged sonication.

As illustrated in Figure 4b, changes in water content produced only minor variations in antioxidant activity compared with the pronounced influence of sample mass. This observation agrees well with the statistical analysis, which indicated that the linear effect of water content was not statistically significant as seen in Table 6. This might be the result of excessive solid loading reducing cavitation efficiency, limiting solvent penetration and hindering mass transfer [60]. The nearly planar surface observed in Figure 4c indicates that the interaction between extraction duration and water content had little influence on antioxidant activity. This finding is supported by the ANOVA results, where neither the BC interaction nor the linear effect of water content was statistically significant (Table 6).

3.6. Optimization Constraints and Optimal Solution

Numerical optimization was performed using the desirability function to maximize TPC and antioxidant activity simultaneously, while keeping all three extraction variables within their experimental ranges (Table 8). The procedure yielded a single optimal solution with an overall desirability of 0.963 (Figure 5). Since desirability values range from 0 to 1, with values closer to 1 indicating a better overall compromise among the selected objectives [61], the obtained result confirms that both responses were satisfactorily optimized. The red markers in Figure 5 indicate the optimal levels of the independent variables, whereas the blue markers represent the predicted response values under the optimum conditions. The optimum extraction conditions were predicted to be a sample mass of 1.09 g, an extraction duration of 24.77 min, and a water content of 38.20%. The predicted response values were 34.55 mg-GAE/g-ADS for TPC and 12.30 mg-TEAC/g-ADS for AA under these conditions (Table 8). To validate the optimization model, extraction experiments were performed under the predicted optimum conditions. The close agreement between the predicted and experimental responses (<2% of deviation) confirms the adequacy of the developed response surface models for optimizing DES-UAE of bioactive substances from pineapple crowns.

However, direct comparison of the TPC and antioxidant activity obtained in the present study with previous reports is challenging. Existing studies have primarily employed conventional extraction systems, and have evaluated antioxidant activity using different analytical methods (DPPH, FRAP, ABTS and ORAC). Moreover, TPC has been reported using different expression bases (such as mg GAE g^{-1} crude extract, mg GAE 100 g^{-1} sample or mg GAE 100 mL^{-1} infusion) [62–64]. These methodological differences limit direct comparison of the reported values. Nevertheless, Azizan et al. identified pineapple crown as the pineapple by-product with the highest phenolic content and antioxidant potential, indicating that this biomass is a promising source of bioactive compounds [62].

Interestingly, Azizan et al. also observed that the extract with the highest TPC did not necessarily exhibit the strongest antioxidant activity, suggesting that antioxidant capacity depends not only on the total amount of phenolic compounds but also on their composition and structural characteristics as explained earlier.

Table 8. Constraints and goals defined for numerical optimization, and the resulting optimal extraction conditions.

Name	Goal	Lower Limit	Upper Limit	Lower Weight	Upper Weight	Importance
A: Sample mass	Is in range	0.5	1.5	1	1	3
B: Duration	Is in range	15	45	1	1	3
C: Water content	Is in range	20	50	1	1	3
TPC	Maximize	24.241	35.184	1	1	3
AA	Maximize	6.071	12.398	1	1	3

Optimal solution						
Sample mass (g)	**Duration (min)**	**Water content (%)**	**Responses**	**Predicted**	**Experimental**	**Error (%)**
1.09	24.75	38.21	TPC (mg-GAE/g-ADS)	34.55	34.66 ± 0.002	<2
			AA (mg-TEAC/g-ADS)	12.30	12.26 ± 0.001	

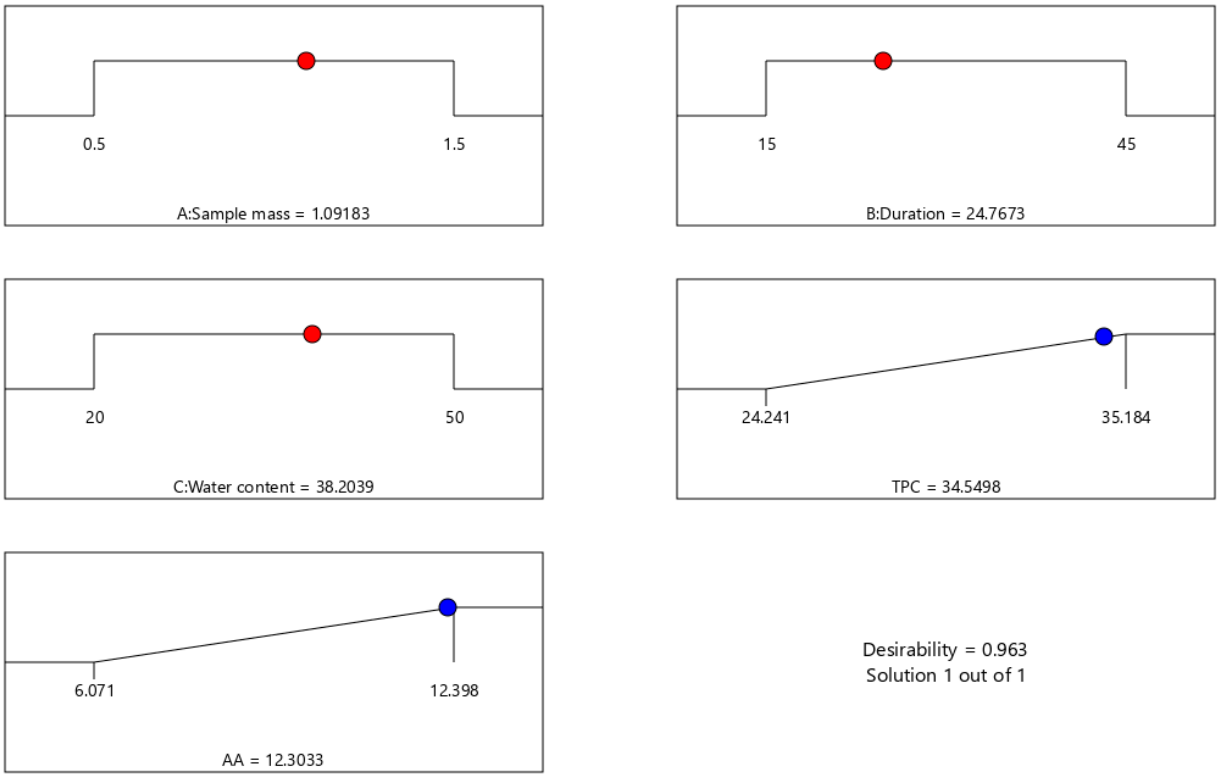

Figure 5. Desirability ramp showing the optimum extraction conditions for simultaneous maximization of total phenolic content (TPC) and antioxidant activity (AA). The red dots indicate the selected optimal values of the extraction factors (sample mass, duration and water content), while the blue dots represent the predicted responses for TPC and AA under the optimized conditions.

Although the proposed DES-UAE approach demonstrated promising extraction performance, several limitations should be acknowledged. The present study did not include chromatographic characterization of the extracted phenolic compounds. Therefore, although TPC and antioxidant activity provided global measures for screening and process optimization, the present data do not permit identification or quantification of individual phenolic constituents or determination of compound-specific extraction selectivity. Future studies employing HPLC-DAD and/or LC-MS/MS should therefore identify and quantify the major phenolic constituents of the optimized extract and evaluate the selectivity of the DES system toward specific phenolic classes.

4. Conclusions

A DES-based ultrasound-assisted extraction strategy was developed to obtain phenolic-rich extracts from pineapple crowns. Among the tested solvents, glycerol/urea (1:1) showed the best overall extraction performance, and 50 °C was selected for process optimization. The optimum conditions were 1.09 g sample mass, 24.75 min extraction time, and 38.21% water content, corresponding to predicted values of 34.66 mg GAE/g-ADS for total phenolic content and 12.30 mg TEAC/g-ADS for antioxidant activity. The quadratic models adequately described the experimental data, with R^2 values of 0.9871 and 0.9906, respectively. FTIR analysis indicated changes in the intermolecular interaction environment of the DES components, while PCA provided a complementary comparison of solvent performance. Taken together, the results support the use of the proposed workflow as a practical approach for the valorization of pineapple crown biomass.

Author Contributions: Conceptualization, S.Ş. and O.C.; methodology, R.N.B., İ.T. and S.Ş.; software, R.N.B.; validation, A.N.E., Z.A.A., R.N.B. and İ.T.; formal analysis, R.N.B. and İ.T.; investigation, A.N.E., Z.A.A., R.N.B. and İ.T.; resources, S.Ş.; data curation, R.N.B. and İ.T.; writing—original draft preparation, S.Ş.; writing—review and editing, R.N.B., İ.T., O.C. and S.Ş.; visualization, R.N.B.; supervision, O.C. and S.Ş. All authors have read and agreed to the published version of the manuscript.

Funding: This research received no external funding.

Data Availability Statement: The data presented in this study are available from the corresponding author upon reasonable request.

Acknowledgments: During the preparation of this manuscript, the authors used OpenAI ChatGPT (GPT-5.5) for language refinement. The authors reviewed and edited the output and take full responsibility for the content of this publication. Rabia Nur Bozkurt gratefully acknowledges the support provided by the TÜBİTAK BİDEB 2211 Domestic Postgraduate Scholarship Program during her doctoral studies.

Conflicts of Interest: The authors declare no conflicts of interest.

References

1. Câmara, J.S.; Perestrelo, R.; Berenguer, C.V.; Andrade, C.F.P.; Gomes, T.M.; Olayanju, B.; Kabir, A.; Rocha, C.M.R.; Teixeira, J.A.; Pereira, J.A.M. Green Extraction Techniques as Advanced Sample Preparation Approaches in Biological, Food, and Environmental Matrices: A Review. *Molecules* **2022**, *27*, 2953. [CrossRef]
2. Meher, A.K.; Zarouri, A. Green Analytical Chemistry—Recent Innovations. *Analytica* **2025**, *6*, 10. [CrossRef]
3. Yadav, S.; Malik, K.; Moore, J.M.; Kamboj, B.R.; Malik, S.; Malik, V.K.; Arya, S.; Singh, K.; Mahanta, S.; Bishnoi, D.K. Valorisation of Agri-Food Waste for Bioactive Compounds: Recent Trends and Future Sustainable Challenges. *Molecules* **2024**, *29*, 2055. [CrossRef]
4. Pal, P.; Singh, A.K.; Srivastava, R.K.; Rathore, S.S.; Sahoo, U.K.; Subudhi, S.; Sarangi, P.K.; Prus, P. Circular Bioeconomy in Action: Transforming Food Wastes into Renewable Food Resources. *Foods* **2024**, *13*, 3007. [CrossRef]
5. Motta, T.; Nogueira, M.F.; Santos, F.; Puga, A.; Fernandes, F.; Correia, M.; Grosso, C.; Soares, C.; Delerue-Matos, C. Pineapple Waste Utilization: Generating Wealth from Waste in a Circular Economy. In *Biorefining Fruit Waste: Technological Advances in a Circular Bioeconomy*; Scrivener Publishing: Beverly, MA, USA, 2025; pp. 325–356.

6. Liao, A.Y.; Spizzirri, E.; Rodriguez-Vasquez, M.J.; Bustamante-Roman, M.; Rojas-Sossa, J.-P.; Toscano, A.; Valenti, F. Powering Pineapple Industry with Pineapple Residues-A Circular Bioenergy Strategy for Costa Rica. *Renew. Energy* **2026**, *266*, 125709. [CrossRef]
7. Saini, R.; Singhania, R.R.; Chen, C.-W.; Patel, A.K.; Saini, J.K.; Chauhan, A.S.; Dong, C.-D. Pineapple Leaves Waste—A Potential Feedstock for Production of Value-Added Products in Biorefinery: Pineapple Leaves Waste Biorefinery. *Indian J. Exp. Biol. (IJEB)* **2023**, *61*, 729–738. [CrossRef]
8. Nogueira, T.B.d.B.; de Farias, P.M.; Bicas, J.L.; Simões Larraz Ferreira, M.; Fai, A.E.C. The Pineapple Crown (*Ananas comosus*): From Agro-Waste to Functional Ingredient and Material. *ACS Food Sci. Technol.* **2026**, *6*, 189–206. [CrossRef]
9. Bansod, S.P.; Parikh, J.K.; Sarangi, P.K. Pineapple Peel Waste Valorization for Extraction of Bio-Active Compounds and Protein: Microwave Assisted Method and Box Behnken Design Optimization. *Environ. Res.* **2023**, *221*, 115237. [CrossRef]
10. Lourenço, S.C.; Campos, D.A.; Gómez-García, R.; Pintado, M.; Oliveira, M.C.; Santos, D.I.; Corrêa-Filho, L.C.; Moldão-Martins, M.; Alves, V.D. Optimization of Natural Antioxidants Extraction from Pineapple Peel and Their Stabilization by Spray Drying. *Foods* **2021**, *10*, 1255. [CrossRef]
11. Vargas-Serna, C.L.; Ochoa-Martínez, C.I.; Vélez-Pasos, C. Microwave-Assisted Extraction of Phenolic Compounds from Pineapple Peel Using Deep Eutectic Solvents. *Horticulturae* **2022**, *8*, 791. [CrossRef]
12. Polanía, A.M.; Londoño, L.; Ramírez, C.; Bolívar, G. Influence of Ultrasound Application in Fermented Pineapple Peel on Total Phenolic Content and Antioxidant Activity. *Fermentation* **2022**, *8*, 314. [CrossRef]
13. Harith, N.S.; Rahman, N.A.; Zamanhuri, N.A.; Hashib, S.A. Microwave-Based Antioxidant Extraction from Pineapple Peel Waste. In *Proceedings of the Materials Today: Proceedings*; Elsevier Ltd.: Amsterdam, The Netherlands, 2023; Volume 87, pp. 126–131.
14. Hu, H.; Zhao, Q. Optimization Extraction and Functional Properties of Soluble Dietary Fiber from Pineapple Pomace Obtained by Shear Homogenization-Assisted Extraction. *RSC Adv.* **2018**, *8*, 41117–41130. [CrossRef]
15. Sanahuja, A.B.; García, A.V.; Baenas, N.; Ferrando, B.O.; Periago, M.J.; Alonso, N.C.; Sánchez, R.; Todolí, J.L. Valorization of Pineapple Core Waste for Sequential Extraction of Phenolic Compounds and Carotenoids: Optimization Through Ultrasound-Assisted Method and Box–Behnken Design. *Food Bioprocess Technol.* **2025**, *18*, 2618–2631. [CrossRef]
16. Hadidi, M.; Amoli, P.I.; Jelyani, A.Z.; Hasiri, Z.; Rouhafza, A.; Ibarz, A.; Khaksar, F.B.; Tabrizi, S.T. Polysaccharides from Pineapple Core as a Canning By-Product: Extraction Optimization, Chemical Structure, Antioxidant and Functional Properties. *Int. J. Biol. Macromol.* **2020**, *163*, 2357–2364. [CrossRef]
17. Gavahian, M.; Chu, R. Ohmic Heating Extraction at Different Times, Temperatures, Voltages, and Frequencies: A New Energy-Saving Technique for Pineapple Core Valorization. *Foods* **2022**, *11*, 2015. [CrossRef]
18. García, A.V.; Martínez, M.I.D.; Landete, M.P.; Moya, M.S.P.; Sanahuja, A.B. Potential of Industrial Pineapple (*Ananas comosus* (l.) Merrill) By-products as Aromatic and Antioxidant Sources. *Antioxidants* **2021**, *10*, 1767. [CrossRef]
19. Wu, L.; Li, L.; Chen, S.; Wang, L.; Lin, X. Deep Eutectic Solvent-Based Ultrasonic-Assisted Extraction of Phenolic Compounds from *Moringa oleifera* L. Leaves: Optimization, Comparison and Antioxidant Activity. *Sep. Purif. Technol.* **2020**, *247*, 117014. [CrossRef]
20. Alasalvar, H.; Yildirim, Z. Ultrasound-Assisted Extraction of Antioxidant Phenolic Compounds from *Lavandula angustifolia* Flowers Using Natural Deep Eutectic Solvents: An Experimental Design Approach. *Sustain. Chem. Pharm.* **2021**, *22*, 100492. [CrossRef]
21. Plaza, M.; Marina, M.L. Natural Deep Eutectic Solvents and Ultrasound-Assisted Extraction for the Recovery of Antioxidant Phenolic Compounds from Orange Pomace. *Microchem. J.* **2025**, *212*, 113366. [CrossRef]
22. Mushtaq, M.; Amin, Q.A.; Wani, T.A.; Hussain, S.Z.; Bhat, T.A.; Parveen, S.; Chaudhary, A.A.; Ali, M.A.; Qadri, T.; Amin, I. Cavitation-Driven Extraction: How Ultrasound-Induced Acoustic Cavitation Maximizes Bioactive Compound Recovery from *S. costus* Roots. *Ultrason. Sonochem.* **2025**, *122*, 107643. [CrossRef]
23. Peng, L.; Gao, X.; Wang, L.; Zhu, A.; Cai, X.; Li, P.; Li, W. Design of Experiment Techniques for the Optimization of Chromatographic Analysis Conditions: A Review. *Electrophoresis* **2022**, *43*, 1882–1898. [CrossRef]
24. Aboushady, D.; Samir, L.; Masoud, A.; Elshoura, Y.; Mohamed, A.; Hanafi, R.S.; El Deeb, S. Chemometric Approaches for Sustainable Pharmaceutical Analysis Using Liquid Chromatography. *Chemistry* **2025**, *7*, 11. [CrossRef]
25. Ghasemi, G.; Fattahi, M.; Alirezalu, A. Screening Genotypes and Optimizing Ultrasonic Extraction of Phenolic Antioxidants from *Rheum ribes* Using Response Surface Methodology. *Sci. Rep.* **2024**, *14*, 21544. [CrossRef]
26. Szpisják-Gulyás, N.; Al-Tayawi, A.N.; Horváth, Z.H.; László, Z.; Kertész, S.; Hodúr, C. Methods for Experimental Design, Central Composite Design and the Box–Behnken Design, to Optimise Operational Parameters: A Review. *Acta Aliment.* **2023**, *52*, 521–537. [CrossRef]
27. Weremfo, A.; Abassah-Oppong, S.; Adulley, F.; Dabie, K.; Seidu-Larry, S. Response Surface Methodology as a Tool to Optimize the Extraction of Bioactive Compounds from Plant Sources. *J. Sci. Food Agric.* **2023**, *103*, 26–36. [CrossRef]
28. Vorobyova, V.; Skiba, M.; Vasyliev, G. Deep Eutectic Solvents: Quantum Chemical Investigation, Thermal Stability and Physicochemical Properties. *Chem. Phys.* **2024**, *586*, 112401. [CrossRef]

29. Kanyairita, G.G.; Mortley, D.G.; Boersma, M.; Collier, W.E. Comparison of the Efficiency of Deep Eutectic and Organic Solvents in the Extraction of Phytochemicals from *Cannabis sativa* L. *Separations* **2024**, *11*, 106. [CrossRef]
30. Casas-Rodríguez, A.D.; Contreras, S.A.C.; González-Martínez, D.W.; Meléndez-Rentería, N.P.; Sáenz-Galindo, A.; Morales-Martínez, T.K.; Ascacio-Valdés, J.A.; Sepúlveda-Torre, L. Evaluation of Process Parameters on Phenolic Recovery and Antioxidant Activity Using Ultrasonic and Microwave-Assisted Extraction from Pineapple Peel. *Processes* **2025**, *13*, 2500. [CrossRef]
31. Bozkurt, R.N.; Kurtulbaş, E.; Toprakçı, İ.; Topraksever, N. Elucidating Deep Eutectic Solvent-Mediated Recovery of Phenolic Compounds From Cubeb Pepper (*Piper cubeba* Lf) and Their Antioxidant Potential. *Nat. Prod. Commun.* **2026**, *21*, 1934578X261468522. [CrossRef]
32. Sevgili, S.Ş.; Bozkurt, R.N.; Kurtulbaş, E.; Toprakçı, İ. Designing a Sustainable Extraction Platform Using Deep Eutectic Solvents: Valorization of Sidr Leaves Into Bioactive-Rich Fractions. *Nat. Prod. Commun.* **2026**, *21*, 1934578X261467196. [CrossRef]
33. Kaba, İ.; Kiliç, B.; Bozkurt, R.N.; Koca, A. Green-Synthesized CuO/Cu2O-Supported g-C3N4 p–n Junction Photocatalyst for Photo (Electro) Catalytic Hydrogen Evolution. *J. Photochem. Photobiol. A Chem.* **2026**, *479*, 117310. [CrossRef]
34. Jollife, I.T.; Cadima, J. Principal Component Analysis: A Review and Recent Developments. *Philos. Trans. R. Soc. A Math. Phys. Eng. Sci.* **2016**, *374*, 20150202. [CrossRef]
35. Ahmadian-Kouchaksaraie, Z.; Niazmand, R.; Najafi, M.N. Optimization of the Subcritical Water Extraction of Phenolic Antioxidants from *Crocus sativus* Petals of Saffron Industry Residues: Box-Behnken Design and Principal Component Analysis. *Innov. Food Sci. Emerg. Technol.* **2016**, *36*, 234–244. [CrossRef]
36. Rout, R.K.; Kumar, A.; Rao, P.S. A Multivariate Optimization of Bioactive Compounds Extracted from Oregano (*Origanum vulgare*) Leaves Using Pulsed Mode Sonication. *J. Food Meas. Charact.* **2021**, *15*, 3111–3122. [CrossRef]
37. Kaba, İ.; Bozkurt, R.N.; Kurt, E.A.; Kerkez-Kuyumcu, Ö.; Koca, A. *Aloe vera*-Derived Ag-Doped TiO_2 Nanoparticles Immobilized by Chitosan Films for Photo(Electro)Catalytic and Antimicrobial Functions. *J. Environ. Chem. Eng.* **2025**, *13*, 120436. [CrossRef]
38. Hanry, E.L.; Redzwan, N.F.M.; Badeges, N.; Surugau, N. Characterization of Biofilms Developed from Alginate Extracted from *Padina* sp. Incorporated with Calcium Chloride ($CaCl_2$). *J. Phys. Conf. Ser.* **2022**, *2314*, 012022. [CrossRef]
39. Zorba, T.; Papadopoulou, E.; Hatjiissaak, A.; Paraskevopoulos, K.M.; Chrissafis, K. Urea-Formaldehyde Resins Characterized by Thermal Analysis and FTIR Method. *J. Therm. Anal. Calorim.* **2008**, *92*, 29–33. [CrossRef]
40. Ishaq, M.; Saeed, U.; Belousov, A.S.; Qamar, S.; Shafique, S.; Afzal, Z.M.; Arshad, I.; Shafiq, I. Performance Tuning of Surface Modified Ceria Based Mixed Matrix Membrane for Effective CO_2 Separation. *J. Appl. Polym. Sci.* **2024**, *141*, e56084. [CrossRef]
41. Bozkurt, R.N.; Şahin, S.; Cadar, O. Green Synthesis of Titanium Dioxide Nanoparticles Using a Deep Eutectic Solvent-Based Extract of *Prunus spinosa* L. for Photocatalytic Degradation of 2,4-Dichlorophenoxyacetic Acid. *Inorg. Chem. Commun.* **2026**, *188*, 116449. [CrossRef]
42. Hashempur, M.H.; Zareshahrabadi, Z.; Shenavari, S.; Zomorodian, K.; Rastegari, B.; Karami, F. Deep Eutectic Solvent-Based Extraction of Rosemary Leaves: Optimization Using Central Composite Design and Evaluation of Antioxidant and Antimicrobial Activities. *New J. Chem.* **2025**, *49*, 4495–4505. [CrossRef]
43. Topraksever, N.; Ozgul Artuc, G. Optimization of VA-NADES-ME for the One-Step Separation and Determination of Rhodamine B and Rhodamine 6G in Red Pencil Samples. *Sep. Sci. Technol.* **2026**, *61*, 837–850. [CrossRef]
44. Hernández-Paredes, J.; Carrillo-Pesqueira, F.J.; Esparza-Ponce, H.E.; Hernández-Negrete, O.; Alvarez-Ramos, M.E. L-Proline–Sodium Nitrate Obtained from Solvent Drop Grinding. *Polyhedron* **2015**, *91*, 84–88. [CrossRef]
45. Kharmawlong, G.K.; Nongrum, R.; Chhetri, B.; Rani, J.W.S.; Rahman, N.; Yadav, A.K.; Nongkhlaw, R. Green and Efficient One-Pot Synthesis of 2,3-Dihydroquinazolin-4(1H)-Ones and Their Anthelmintic Studies. *Synth. Commun.* **2019**, *49*, 2683–2695. [CrossRef]
46. Balaž, F.; Bojić, A.; Arapović, K.; Petrović, A.T.; Grujić-Letić, N.; Gligorić, E.; Teofilović, B. Innovative Green Extraction of Phenolic Compounds from Chicory (*Cichorium intybus*) Using Natural Deep Eutectic Solvents. *Period. Polytech. Chem. Eng.* **2025**, *69*, 537–544. [CrossRef]
47. Liu, J.Z.; Lu, X.X.; Yang, X.T.; Jiang, L.J.; Cui, Q. An Efficient Approach for the Extraction of Polyphenols from Pomegranate Peel Using the Green Solvent and Profiling by UPLC-Q-TOF-MS/MS Analysis. *Microchem. J.* **2024**, *205*, 111421. [CrossRef]
48. Vidić, M.; Grujić-Letić, N.; Teofilović, B.; Gligorić, E. Towards a Green and Sustainable Valorization of *Salix amplexicaulis*: Integrating Natural Deep Eutectic Solvents and Microwave-Assisted Extraction for Enhanced Recovery of Phenolic Compounds. *Sustainability* **2025**, *17*, 6347. [CrossRef]
49. L Nascimento, L.; dos Santos, P.N.A.; Albuquerque, L.; Pita, B.L.d.M.; de Almeida, L.S.; de Oliveira, M.L.; Moreira, C.d.A.; Teixeira, F.R.P.; Caramão, E.B.; Dias, F.d.S.; et al. Ultrasound-Assisted of Methylxanthines from Cocoa Bean Shells Using Glycerol–Urea Natural Deep Eutectic (NADES): Optimization and Greenness Assessment. *ACS Omega* **2025**, *10*, 44064–44076. [CrossRef]
50. Li, H.; Guo, X.; He, X.; Liu, J.; Han, M.; Chen, M.; Li, X.; Ren, X. Deep Eutectic Solvent-Based Extraction and Recovery of Phenolic Compounds: From Conventional Media to Switchable Recovery Strategies. *Microchim. Acta* **2026**, *193*, 607. [CrossRef]
51. Jacobo-Velázquez, D.A.; Cisneros-Zevallos, L. Correlations of Antioxidant Activity against Phenolic Content Revisited: A New Approach in Data Analysis for Food and Medicinal Plants. *J. Food Sci.* **2009**, *74*, R107–R113. [CrossRef]

52. Uribe, E.; López, J.; Vega-Galvez, A.; Mejias, N.; Hidalgo, P.; Pasten, A. Drying Kinetics and Variations in Chemical and Antioxidant Properties of Cauliflower (*Brassica oleracea* L. var. *botrytis*) at Different Vacuum Drying Temperatures. *Processes* **2026**, *14*, 1336. [CrossRef]
53. Morris, M.D. A Class of Three-Level Experimental Designs for Response Surface Modeling. *Technometrics* **2000**, *42*, 111–121. [CrossRef]
54. López-Díaz, P.E.; Torres-Aguilar, H.; Solano, R.; Lagunez-Rivera, L. Optimization of Green Pressurized Liquid Extraction of Phenolic Compounds with Inhibitory Capacity Reactive Oxygen Species from *Crescentia alata* Using a Box-Behnken Design. *Separations* **2025**, *12*, 331. [CrossRef]
55. Paulo, F.; Tavares, L.; Santos, L. Response Surface Modeling and Optimization of the Extraction of Phenolic Antioxidants from Olive Mill Pomace. *Molecules* **2022**, *27*, 8620. [CrossRef]
56. Joey, N.L.; Ismail, N.A.; Mokhtar, A.M.A.; Zain, M.S.C. Integrated Ultrasonic–Natural Deep Eutectic Solvent-Assisted Extraction for Standardizing Polyphenol-Enriched Extract from Cocoa (*Theobroma cacao* L.) Rind with Enhanced Antioxidant Properties. *J. Food Meas. Charact.* **2026**, *20*, 357–375. [CrossRef]
57. Singh, S.M.; Tripathy, S.; Srivastav, P.P. Bioactive Compound Extraction from Giloy Leaves and Steam Using Ultrasound: Bioactivity, Antimicrobial, and LC–MS/MS Study: SM Singh et al. *Food Sci. Biotechnol.* **2025**, *34*, 1835–1847.
58. Kalkan, E.; Maskan, M. Optimization of Sonication and Homogenization-Assisted Solvent Extraction of Cottonseed Oil Using RSM: Oil Recovery, Antioxidant Properties, and Oxidative Stability. *J. Food Process Eng.* **2025**, *48*, e70125. [CrossRef]
59. Zabot, G.L.; Viganó, J.; Silva, E.K. Low-Frequency Ultrasound Coupled with High-Pressure Technologies: Impact of Hybridized Techniques on the Recovery of Phytochemical Compounds. *Molecules* **2021**, *26*, 5117. [CrossRef]
60. Sahlan, M.; Rosarina, D.; Ratna Suminar, H.F.; Diatama Pohan, Y.; Hidayatullah, I.M.; Narawangsa, D.R.; Putri, D.N.; Sari, E.; Perdani, M.S.; Wibowo, Y.G.; et al. Microwave–Ultrasound-Assisted Extraction Coupled with Natural Deep Eutectic Solvent Enables High-Yield, Low-Solvent Recovery of Curcumin from *Curcuma longa* L. *Pharmaceutics* **2025**, *17*, 818. [CrossRef]
61. 5.5.3.2.2. Multiple Responses: The Desirability Approach. Available online: https://www.itl.nist.gov/div898/handbook/pri/section5/pri5322.htm?utm_source=chatgpt.com (accessed on 25 July 2026).
62. Azizan, A.; Lee, A.X.; Hamid, N.A.A.; Maulidiani, M.; Mediani, A.; Ghafar, S.Z.A.; Zolkeflee, N.K.Z.; Abas, F. Potentially Bioactive Metabolites from Pineapple Waste Extracts and Their Antioxidant and α-Glucosidase Inhibitory Activities by 1H NMR. *Foods* **2020**, *9*, 173. [CrossRef]
63. Braga de Brito Nogueira, T.; Souza da Silva, L.; Araujo Lima, C.F.; Carvalho, M.G.d.O.; Marques, M.R.d.C.; Felzenszwalb, I.; Bicas, J.L.; Ferreira, M.S.L.; Fai, A.E.C. Transforming Waste into a Bioactive Resource: Phenolic Profile, Antioxidant, and Antimutagenic Properties of Pineapple (*Ananas comosus*) Crown Infusion. *Sustain. Food Technol.* **2026**, *4*, 1115–1125. [CrossRef]
64. Zampar, G.G.; Zampar, I.C.; Beserra da Silva de Souza, S.; da Silva, C.; Bolanho Barros, B.C. Effect of Solvent Mixtures on the Ultrasound-Assisted Extraction of Compounds from Pineapple by-Product. *Food Biosci.* **2022**, *50*, 102098. [CrossRef]